Published in final edited form as:

Am J Transplant. 2012 October ; 12(10): 2641–2651. doi:10.1111/j.1600-6143.2012.04181.x.

Patterns of *De Novo* Allo B Cells and Antibody Formation in Chronic Cardiac Allograft Rejection After Alemtuzumab Treatment

J. Kwun[a], **B. C. Oh**[a], **A. C. Gibby**[a], **R. Ruhil**[a], **V. T. Lu**[a], **D. W. Kim**[a], **E. K. Page**[a], **O. P. Bulut**[a], **M. Q. Song**[a], **A. B. Farris**[b], **A. D. Kirk**[a], **S. J. Knechtle**[a,*,†], and **N. N. Iwakoshi**[a,†]

[a]Emory Transplant Center, Department of Surgery, Emory University School of Medicine, Atlanta, GA

[b]Department of Pathology, Emory University School of Medicine, Atlanta, GA

Abstract

Even though the etiology of chronic rejection (CR) is multifactorial, donor specific antibody (DSA) is considered to have a causal effect on CR development. Currently the antibody-mediated mechanisms during CR are poorly understood due to lack of proper animal models and tools. In a clinical setting, we previously demonstrated that induction therapy by lymphocyte depletion, using alemtuzumab (anti-human CD52), is associated with an increased incidence of serum alloantibody, C4d deposition and antibody-mediated rejection in human patients. In this study, the effects of T cell depletion in the development of antibody-mediated rejection were examined using human CD52 transgenic (CD52Tg) mice treated with alemtuzumab. Fully mismatched cardiac allografts were transplanted into alemtuzumab treated CD52Tg mice and showed no acute rejection while untreated recipients acutely rejected their grafts. However, approximately half of long-term recipients showed increased degree of vasculopathy, fibrosis and perivascular C3d depositions at posttransplant day 100. The development of CR correlated with DSA and C3d deposition in the graft. Using novel tracking tools to monitor donor-specific B cells, alloreactive B cells were shown to increase in accordance with DSA detection. The current animal model could provide a means of testing strategies to understand mechanisms and developing therapeutic approaches to prevent chronic rejection.

Keywords

Allo-B cell; alloantibody; chronic rejection; T cell depletion; Alemtuzumab

Introduction

Chronic rejection (CR) of organ transplants remains an unsolved problem in the field of transplantation and is the major reason for late graft failure (1,2). The etiology of CR is

*Corresponding author: Stuart J. Knechtle, stuart.knechtle@emoryhealthcare.org.
†SJK and NI share last authorship for this work.

Disclosure

The authors of this manuscript have no conflicts of interest to disclose as described by the *American Journal of Transplantation*.

often described as “multifactorial” and poorly understood (3,4). Pathologically, common features of CR include vasculopathy leading to ischemic injury, and fibrosis associated with replacement of normal tissue architecture by fibrous elements. Each transplanted solid organ type develops manifestations of CR unique to that organ, but fibrosis and vasculopathy are common to all. Antibody-mediated injury has been suggested as the leading cause of CR in humans based on longitudinal studies of kidney, lung, and heart transplant recipients (5–8). The diagnosis of antibody-mediated rejection (AMR) in kidney transplantation has been clearly defined as the presence of allograft injury by histology, donor-specific antibody in blood, and C4d peritubular capillary staining (9). Despite prevailing evidence of HLA antibodies associated with CR in human patients (5,10), animal models addressing the role of B cells and antibody in the development of cardiac allograft vasculopathy (CAV) are controversial (11,12). It is generally accepted that T cells play a central role in CAV development (13,14), but less is known about *de novo* B cell responses following transplantation.

Recent recognition of the higher incidence of humoral rejection following lymphocyte depletion with alemtuzumab in certain human immunosuppressive protocols (15–17) has generated interest in studying the mechanisms by which lympohocyte depletion mediates DSA formation in clinically relevant settings. The goal of the present study was to mimic lymphocyte depletion induced humoral anti-donor responses and CAV development after murine heart transplantation. The significance of this work is in defining the relationship of DSA and CAV using a discriminating model in which potential interventions in this pathological process can be studied.

Material and Methods

Animals and heart transplantation

Homozygous huCD52Tg (H-2^K) mice were kindly donated by Herman Waldman (18). C57BL/6 mice were purchased from the Jackson Laboratory (Bar Harbor, ME). Mice were housed in a specific pathogen-free barrier facility and used at 6–12 weeks of age. C57BL/6 (H-2^b) donor hearts were transplanted into CD52Tg (H-2^k) recipients using a modified technique of the methods described by Corry et al. (19). To induce T cell depletion *in vivo*, 10μg alemtuzumab (in 200μl PBS) was intraperitoneally administered on days −2, −1, +2, and +4 of transplantation. The grafts were monitored by daily palpation and graded from 4+ (strong beat) to 0 (no beat), which was confirmed by laparotomy at the time of sacrifice. The Emory University Animal care and Use Committee approved all studies.

Flow cytometry

Fixative-Free Lysing solution (Invitrogen, MD) was applied to whole blood according to the manufacturer’s instructions. PBMC were isolated and placed into a single cell suspension in FACS buffer (PBS containing 2% FBS and 0.09% NaN_3). Spleen was recovered on the designated day and placed into single cell suspension by passing through a cell strainer (BD labware, Franklin Lakes, NJ, USA). Lymphocytes were counted using a hemocytometer under a light microscope. Cells were resuspended in FACS buffer and stained with FITC, PE, PerCp Cy 5.5, PE-Cy7, Pac Orange, Pac Blue, APC, or APC-Cy7 conjugated antibodies

directed at mouse CD4, CD8, CD25, FoxP3, CD44, CD62L for T cells and GL7, IgG, IgM, IgD, CD38, CD94, CD4/CD8/F4/80 (Dump) for B cells (BD Pharmingen, San Diego, CA, USA). Syngeneic (H-2K^k/D^k) and allogenic (H-2K^b/D^b) MHC monomers were generated from NIH tetramer facility. Monomers were tetramerized with Streptavidin-APC and Streptavidin-APC-Cy7 respectively. Flow cytometry data were collected on a BD FACSCaliber or BD FACS LSRII bench-top analyzer (BD Bioscience, San Jose, CA, USA) and analyzed using FlowJo software (Tree Star, Ashland, OR, USA).

Detection of donor-specific antibody (DSA)

Flow cross match was performed using naïve CD52Tg, pretransplant recipient, as well as posttransplant recipient serum. C57BL/6 splenocytes (1×10^6) were re-suspended and incubated with equal volume of fetal bovine serum (FBS; 10 minute blocking), then washed with PBS containing 2% FBS and 0.09% NaN_3. Recipient serum (1:32 dilution) was incubated with donor splenocytes for 20 min at 4°C in the dark. 5 μl of FITC-conjugated anti-mouse Ig was added to the samples and incubated for 20 min after washing. The T cells were stained with APC-conjugated anti-CD3. Samples were analyzed on a FACScaliber (Beckman Coulter, Brea, CA, USA) or LSR II (Beckman Coulter). The alloantibody production of each serum sample was calculated as fold increase compared to the negative control in the same test run.

Immunohistochemistry

The grafts from long-term recipients were recovered on day 100 or 200 after transplantation. The explanted grafts were bisected sagitally and fixed in 10% formalin or frozen. For immunohistochemical staining, sections were blocked for nonspecific staining using 10% normal donkey serum in TBS (Tris buffered saline) with 1% BSA for 1 hour followed by 5% non-fat milk in PBS, 30 minutes. Rat anti-mouse primary antibodies against T cell markers CD3 (BD Pharmingen) were incubated overnight at 4°C. Endogenous peroxidase quenching was performed postprimary antibody incubation with 1% hydrogen peroxide in TBS for 10 minutes. A donkey anti-rat IgG-horeseradish peroxidase (HRP) conjugated secondary antibody from Jackson Laboratories was used for detection and incubated for 45 minutes at room temperature. The signal was visualized using diaminobenzidine (DAB) chromogen (DakoCytomation, Carpinteria, CA, USA) followed by counterstaining with hematoxylin.

Morphometric analysis

Whole slide of grafts stained with elastic and trichrome were scanned with an Aperio ScanScope XT (Aperio Technologies, Inc., Vista, CA, USA) from CD52Tg recipients and analyzed using the ImageScope (Aperio Technologies) for morphometric analysis. Scanned images of all vessels in a plane were analyzed and measured with computer-based software (Aperio Technologies). Neointimal hyperplasia was calculated ([intima area/(lumen+intima area)] × 100) from captured vessels for each graft. Data are expressed as mean ± SEM of six grafts in each group. Vessels with a neointimal hyperplasia over 20% were considered as diseased vessels. Their presence was expressed as a percentage for each graft. For fibrosis and T cell infiltration, trichrome stained and anti-CD3 mAb stained sections were scanned with an Aperio ScanScope XT and analyzed using the Image Scope Positive Pixel Count algorithm (20,21). For trichrome and CD3 staining, hue values for blue and brown were

measured in all cases, and average hue for the trichrome (0.64) and CD3 (or HRP/DAB) (0.1) were used when evaluating these stains. A pathologist (A.B.F) with expertise in transplant pathology viewed C3d, H&E, elastic, and trichrome stained slides under a light microscope. C3d, fibrosis and vasculopathy were scored semi-quantitatively.

Measuring anti-donor response using MLR

IFN-γ producing cell numbers in response to donor stimulation were quantified with ELISPOT assay as previously described (22). Briefly, anti-mouse IFN-γ Ab (R&D Systems, Minneapolis, MN, USA) was incubated at 5μg/ml in PBS at 4°C over night in 96-Well MultiScreen-HA Filter Plates (Milipore, Bedford, MA, USA). 5×10^5 splenocytes from alemtuzumab-treated or untreated CD52Tg mice recipients on day 100 after heart transplantation or age matched naïve CD52Tg mice were co-cultured with equal numbers of irradiated (2000 rad) donor splenocytes for 48 hours at 37°C.

Biotinylated anti-mouse IFN-γ Ab (R&D systems) was used for secondary followed by Streptavidin-alkaline phosphatase (1: 500 dilution; R&D Systems). Spots were visualized with the BCIP/NBT chromogen (R&D Systems). Each spot represented an IFN-γ secreting cell, and the spots were enumerated using an ImmunoSpot Analyzers (Cellular Technology Limited, OH, USA).

Statistics

Experimental results were analyzed by a GraphPad Prism (GraphPad Software 4.0, San Diego, CA, USA) or IBM SPSS Statistics 19 (IBM, Chicago, IL, USA) using the log-rank test for differences in graft survival, Mann-Whitney *U* test for data with grades (semi-quantification), and unpaired Student's *t*-test for other data. All data are presented as mean ± SEM or as indicated. Asterisks denote the significance level determined. Values of p less than 0.05 were considered to be statistically significant. NS indicates no statistical difference ($p > 0.05$).

Results

Profound T cell depletion and long-term cardiac allograft survival after alemtuzumab treatment

CD52 Tg mice express human CD52 under the direction of the mouse CD2 promoter, allowing selective T cell depletion with monoclonal antibody reactive to human CD52, alemtuzumab (or Campath-1H). Both $CD4^+$ and $CD8^+$ T cells are depleted upon treatment with alemtuzumab. Profound depletion of peripheral T cells was achieved after two doses (Figure 1B). In addition, repopulating T cells showed more "memory/effector" phenotype indicated by a $CD44^{hi}CD62L^{lo}$ profile (Figure 1C). Mouse T cells repopulate to baseline levels (as% of lymphocytes) by 10 weeks after transplantation (Figure 1D). Alemtuzumab-treated recipients did not show any graft rejection (Figure 1E; MST > 200 days) despite complete T cell repopulation, while untreated CD52Tg recipients acutely rejected B6 hearts, showing a high intensity of infiltrating mononuclear cells (MNC), severe edema and myocyte damage (MST = 8.0 days; n = 12). Posttransplant date-matched (POD10) alemtuzumab-treated CD52 Tg recipients showed no sign of posttransplant dysfunction

(Figure 1F) with absence of T cell infiltration in the allograft (data not shown). These data indicate that T cell depletion with alemtuzumab prevents acute rejection and promotes long-term survival.

Posttransplant alloantibody production after alemtuzumab treatment

To verify that alemtuzumab-mediated T cell depletion promotes posttransplant alloantibody production, serum samples were analyzed from CD52Tg cardiac allograft recipients. We used a flow cross-match test and donor C57BL/6 splenocytes with serially drawn serum samples from the recipients for measuring donor-specific antibodies (DSA). Serum samples were diluted (1:32 in PBS) and co-cultured with donor splenocytes. Untreated CD52Tg recipients developed serum alloantibody at 2 weeks and maintained high serum alloantibody level. We found that alemtuzumab treatment successfully suppresses alloantibody responses at early time points (Figure 2A). However, 50% of alemtuzumab-treated recipients showed elevated DSA levels (>2 fold; DSA+) compared to pretransplant serum level while the other 50% showed no elevation of DSA (<2 fold; DSA–) at posttransplant day 100 (Figure 2B). As shown in Figure 2C, DSA levels started showing significant differences at 7 weeks posttransplant between the retrospectively separated two groups. Since high levels of DSA were present in 50% of alemtuzumab treated recipients, we evaluated intragraft C3d deposition from DSA+ vs. DSA– recipients at 100 days posttransplant. As shown in Figure 2D, there was clear deposition of C3d at the arterial endothelium and capillaries for both DSA+ and DSA– groups. The presence of C3d staining in the DSA– recipients could represent a low level DSA or complement fixing nondonor specific antibody (e.g., anti-endothelial/angiotensin, etc). However, quantification of C3d from the entire graft showed an elevated level of C3d deposition from DSA+ recipients (Figure 2D and E).

Chronic rejection in alemtuzumab-treated long-term recipients

Even with DSA production, alemtuzumab treated recipients did not show compromised graft function (Figure 1F). To determine the histologic status of allografts, these hearts were explanted 100 days after transplantation. Heart sections were examined for myocyte damage, graft infiltrating cells, and degree of CR. Syngeneic control grafts retained normal microscopic and histologic morphology and were indistinguishable from native hearts. DSA + recipients showed obvious narrowing of vascular lumina due to intimal thickening, a characteristic of CAV at POD100 without profound mononuclear cell infiltration (Figure 3A). Pathological grading performed blindly showed significantly increased vasculopathy from DSA+ recipients (Figure 3B). To quantify CR, we performed morphometric analysis using an Aperio ScanSope XT. The mean neo-intimal hyperplasia values (occlusion%) of the individual hearts within each group were compared between DSA+ vs. DSA– groups. Elastic (or elastic trichrome) staining was used to visualize luminal occlusion and revealed neo-intimal hyperplasia from the DSA+ recipients at day 100, while DSA– recipients showed minimal signs of neo-intimal hyperplasia (<20%). The proportion of diseased vessels (%) for individual grafts was significantly different between DSA+ vs. DSA– recipients (47.58 ± 7.89 vs. 11.50 ± 6.88%, $p < 0.05$; Figure 3C). The degree of luminal occlusion was 38.48 ± 5.5% (n = 6) for DSA+ recipients and 8.432 ± 5.3% (n = 6) for DSA– recipients ($p < 0.01$; Figure 3D). Trichrome (or elastic trichrome) staining revealed development of fibrosis in the graft at day 100 (Figure 3E). DSA+ recipients showed higher

pathological grades in fibrosis score for mycardium ($p < 0.05$; Figure 3F), while endocardium and epicardium did not show any difference (data not shown). Total fibrosis measured by Aperio Scansope also showed significantly increased fibrosis in DSA+ recipients compared to DSA– recipients (41.13 ± 6.12% vs. 20.87 ± 1.53%, $p < 0.05$; Figure 3G). These data suggest that formation of DSA after alemtuzumab treatment promotes CAV and fibrosis without disrupting the quality of the heart beat at 100 days.

The effect of T cells on cardiac allograft vasculopathy (CAV)

Although DSA correlated with development of CR, it was unclear whether this might also be due to differences in T cell-mediated injury between the two groups. We evaluated T cell infiltration in the graft since T cells can mediate CR directly (23–25). As of day 100, there was only minimal perivascular infiltration of T cells in the graft for both DSA+ and DSA– groups (Figure 4A). Visual evaluation of T cell infiltration using morphometric analysis showed no difference of T cell infiltration in the entire graft tissue (atrium excluded) (10.78 ± 3.52 vs. 13.59 ± 3.84%, $p > 0.05$; Figure 4B) as well as in the different compartments including interstitial (1.16 ± 0.16 vs. 1.66 ± 0.33; $p > 0.05$), vascular (0.5 ± 0.34 vs. 0.66 ± 0.33; $p > 0.05$) and quilty areas (1.17 ± 0.98 vs. 1.0; $p > 0.05$) of the allograft (Figure 4C). This indicates that graft-infiltrating T cells are not the confounding factors for CR in this model. We next investigated the contribution of alloreactive T cell function. The role of Th1 cells and Th1 cytokines, especially IFN-γ, has been shown in CR (23,26). The frequency of alloreactive T cells expressing IFN-γ in MLR was assessed by ELISPOT (Figure 4D). Similar numbers of IFN-γ producing cells were noted after ConA (0.05 μg/mL) stimulation among naïve, untreated and alemtuzumab treated groups. However, alemtuzumab treated recipients showed lower levels of IFN-γ producing cells upon allogeneic stimulation compared to untreated recipients (19.50 ± 7.587 vs. 65.17 ± 15.49 cells/well; $p < 0.05$). ELISPOT data suggests that T cells are fully repopulated 100 days after alemtuzumab treatment; however, repopulated T cells are not responsive to donor stimulation. Thus induction of stable long-term graft acceptance after alemtuzumab treatment is associated with T cell hyporesponsiveness.

Alloreactive B cells after T cell depletion

Even though much attention has been devoted to detecting and characterizing DSAs, the B cell subsets that produce DSAs are poorly characterized. In this study, we used a novel tracking method for alloreactive B cells using H-K^b/D^b tetramers fluorescently labeled that bind the donor-specific B cell antigen receptor (BCR). Briefly, lymphocytes were selected for Doublet-, CD4/8/F4/80$^-$ (Dump) and far yellow$^-$ (dead) cells. B cells were separated as CD19$^+$ syngeneic tetramer$^-$ and were further gated against allospecific tetramer Tet B (H-2^b) and IgD (Figure 5A). The H-2 binding reactivity to B cells was peptide independent (Data not shown). As shown in Figure 5(A) (lower panel), anti-donor B cells were not found in syngeneic or third party heart transplant recipients (or naïve untransplanted recipients) at any time point, but were dramatically increased in cardiac allograft recipients starting 3 weeks after transplantation. Tetramer$^+$ B cells from the allograft recipient splenocytes showed an activated B cell phenotype (GL7$^+$ CD95$^+$IgG$^+$B220$^+$; Figure 5B). As shown in Figures 5(C) and (D), H-2K^b/D^b tetramer$^+$ allo-B cells were significantly increased in untreated CD52 cardiac allograft recipients while DSA–recipients (0.041 ± 0.007 vs. 0.006 ± 0.001%; $p <$

0.01) maintained low levels of allo-B cells (as in untransplanted mice) at day 100. DSA+ recipients showed even higher levels of allo-B cells in the spleen compared to untreated recipients (0.124 ± 0.023 vs. 0.041 ± 0.007; $p < 0.01$). Although increased levels of allo-B cells ($IgD^{lo}TetB^{+}CD19^{+}$) were found in the untreated and DSA+ recipients' splenocytes, these allo-B cells showed different phenotypes with respect to CD38 expression at day 100. As shown in Figure 6, allo-B cells from DSA+ recipients showed increased $CD38^{-}$ allo-B cell population representing ongoing germinal center reaction while the untreated recipients showed less $CD38^{-}$ allo-B cells (0.101 ± 0.007 vs. 0.01 ± 0.004; $p < 0.001$). This data suggest that B cells respond continuously to a functioning donor allograft in DSA+ recipients whereas B cells differentiate into memory states in untreated recipients with a rejected graft (without ongoing B cell response).

Stability of chronic rejection phenotype after alemtuzumab treatment

To evaluate the progression of the CR after alemtuzumab treatment, we investigated recipients at day 200. First, we evaluated serum DSA levels using as a cut off an MFI shift of more than twofold. As shown in Figure 7(A), the ratio of the DSA+ vs. DSA– phenotype was unchanged in that 7 out of 15 showed higher alloantibody production while the others showed low titer of the alloantibody (7.41 ± 1.38 vs. 1.4 ± 0.14, $p < 0.01$; Figure 7A). The alloantibody titer was significantly increased at day 200 (7.41 ± 1.38 fold increased) compared to day 100 (3.72 ± 1.38 fold increased) measured from DSA+ recipients of each time point ($p < 0.05$). This shows that DSA production may rise in DSA+ recipients over time. Again, CR was evaluated with H&E, trichrome and elastic (or elastic trichrome) staining of explanted grafts at day 200 (Figure 7B). Graft T cell infiltration was not different in DSA– versus DSA+ cardiac allografts. A significantly increased proportion of diseased vessels (%) was identified in DSA+ recipients at day 200 compared to DSA– recipients (76.08 ± 8.58 vs. 20.76 ± 16.23; $p < 0.05$) or DSA+ recipients at day 100 (76.08 ± 8.58 vs. 47.58 ± 7.89; $p < 0.05$). Neo-intimal hyperplasia (%) was also significantly increased in DSA+ recipients at day 200 compared to DSA– recipients at day 200 (53.14 ± 8.65% vs. 14.27 ± 12.89; $p < 0.05$). However, neointimal hyperplasia did not differ between DSA+ recipients at day 100 (38.48 ± 5.5%; $p > 0.05$). Again, trichrome staining of DSA+ recipients at day 200 did not show significantly elevated total fibrosis compared to DSA– recipients at day 200 or DSA+ recipients at day 100 (Figure 7C). Finally, we observed increased levels of alloreactive B cells from DSA+ recipients at day 200 (0.09 ± 0.02 vs. 0.02 ± 0.004; $p < 0.05$). Alloreactive B cells showed identical phenotypes that were seen at day 100 (Figure 7D). This data suggests that despite continuous deterioration once CAV develops, the CR phenotype might not be gradually increased over time whereas onset of the disease might be previously decided.

Discussion

A major cause of chronic allograft vasculopathy is antibody-mediated injury, which occurs despite the use of current immunosuppressive drugs (5). Antibody-mediated injury may occur as a result of indirect antigen presentation in which donor antigen is presented by recipient antigen-presenting cells (APC) to host immune cells. Upon receiving $CD4^{+}$ T cell help, naïve B cells are activated, differentiate, and eventuate in donor specific antibody

(DSA). In previously reported CR models, alloantibody or B cells contributed little if any to CR (11,27). Such CR models are “acute rejection-driven” (28). Although posttransplant T cell responses may be effectively controlled by current immunosuppresants, the ineffectiveness of the same agents against B cell responses has become apparent. In order to observe CR caused by alloreactive B cell activation, posttransplant alloreactive T cell function must be managed.

The use of alemtuzumab in CD52Tg mice (Figure 1A) induced complete peripheral T cell depletion and promoted long-term cardiac allograft survival without posttransplant graft dysfunction. T cell mediated injury was well controlled during T cell repopulation despite proportionally increased memory T cells (Figure 1). Just as increased antibody-mediated injury may occur in humans after alemtuzumab treatment (16, 17, 29) the mice also developed alloantibody. The rapid DSA production observed at 1–2 weeks after heart transplantation in untreatment was completely abolished after alemtuzumab treatment. Surprisingly, approximately 50% of alemtuzumab treated recipients showed increased serum DSA level at 100 days after transplantation. DSA+ recipients showed elevated pathological C3d deposition in their grafts at day 100 compared to DSA– recipients. These groups segregated as early as 7 weeks (Figure 2). Posttransplant day 100 cardiac grafts revealed increased vasculopathy, neo-intimal hyperplasia and extensive fibrosis exclusively in DSA+ recipients (Figure 3). On the contrary, intragraft T cells were not different between DSA− and DSA+ groups. In addition, IFN-γ producing donor reactive cells measured in mixed lymphocyte reaction suggest T cell hyporesponsiveness in alemtuzumab treated recipients at day 100. Taken together, DSA is the discriminating factor for CAV development in stable long-term grafts associated with lack of anti-donor Th1 cell response. Recently, a distinct subset of helper T cells, follicular helper T cells (Tfh), have been described more specialized T-helper cell phenotype aiding in humoral responses (30). To completely rule out the role of T cells in this phenomenon, Tfh pathways should be further elucidated. Furthermore, in murine and humans studies, a subset of CD4+CD25+FoxP3+ regulatory T cells located within the follicle has been identified. (31–33). These cells may play a critical role in moderating Tfh function. In this regard, it would also be interesting to examine the requirement of the Tfh and their regulatory T cell counterparts in antibody-mediated CR.

To address the potential mechanism by ongoing B cell activation are eventuating in alloantibody production and contributing to CAV in DSA+ recipients, we examined the extent of allo-MHC tetramer^{+} B cells in the spleen of DSA+ and DSA– recipients. Allo-specific B cells ($IgD^{lo}TetB^{+}CD19^{+}$) were identified from spleen after full MHC mismatched cardiac allografts. Phenotypic analysis of allo-specific B cells revealed that these donor MHC tetramer^{+} cells were predominantly activated and isotype-switched effector (GL7, CD95, IgG) B cells. Interestingly, allo-specific B cells were significantly increased only in DSA+ recipients in alemtuzumab-treated recipients (Figure 5). To our knowledge, this is the first demonstration that the development of endogenous allo-specific B cells directly correlates with alloantibody production and CR after heart transplantation. DSA– recipients showed low frequencies of allo-specific B cells with predominantly IgM isotype (Data not shown). Elevated allo-B cells were also found in untreated CD52Tg recipients (Figure 5). Based on the DSA production, allo-B cells are expected to form earlier and to contract at day 90 after acute graft rejection in untreated recipients. In mice, CD38 expression is down-

regulated on germinal center B cells (34). $CD38^{-}$ allo-B cells present exclusively in DSA+ recipients suggest continuous Ag-stimulated germinal center formation (Figure 6). These data suggest that the production of alloantibody is derived from differentiation of donor-specific B cells with relatively distinct phenotypic and functional signatures during CR development.

We evaluated alemtuzumab-treated recipients at day 200 to determine whether the proportion of recipients developing CR gradually increased. If CR were a gradual *de novo* B cell response that depends on T cell repopulation, all recipients should become DSA+ over time. Surprisingly, the incidence of the DSA production at day 200 showed a similar ratio of DSA– to DSA+ recipients (DSA– < 2-fold < DSA+) compared to day 100. The alloantibody levels in DSA+ recipients dramatically increased, but alloantibody levels in DSA– recipients remained low (Figure 7A). We confirmed increased CAV affected vessels and increased alloreactive B cell formation at day 200 while the graft infiltrating T cell number was unchanged between DSA–and DSA+ groups. It is notable that a low level of CR developed even in DSA– recipients. Thus, factors other than DSA contribute to CR even in this model. Alternatively, an undetectable level of DSA may cause CR in our DSA– recipients over time. Currently, we are obtaining more information on this DSA low population showing fold increase between 1.5 and 2.0. The role of low-level alloantibodies needs to be further investigated. Maintenance of a constant ratio of DSA producing phenotypes at day 200 suggests that onset of CR might be determined early after alemtuzumab treatment and that the therapeutic window for possible intervention could be narrow.

The target of alemtuzumab (CD52) is broadly expressed on human leukocytes and their precursors so that treatment with alemtuzumab leads to profound and broad suppression of leukocyte numbers (35). The mouse model used in this study alemtuzumab only depletes T cells since the CD2 promoter has been used for human CD52 transfection (18, 36). We observed only T and NKT cell depletion upon alemtuzumab treatment while B cells, NK cells and monocytes were unaffected (Data not shown). It is notable that T cell depletion in a mouse transplant model mimics the clinical outcome of human patients. Continuous *de novo* emergence of allo-B cells with donor-specific effector function (alloantibody) causes CR in the absence of T cell-mediated rejection.

Acknowledgments

This work was supported by the CHOA Pediatric Liver Transplant Research Program Support (to SJK) and Roche Transplant Research Foundation (ROTRF) Grant 962141545 (to NII). We thank Dr. Christian P. Larsen (Emory University, Department of Surgery) for insightful suggestions on the study. The authors also would like to thank Drew Roenneburg (University of Wisconsin, Department of Surgery) for assistance in immunohistochemistry.

Abbreviations

Ab	antibody
Ag	antigen
APC	antigen presenting cell
BSA	bovine serum albumin

°C	degree(s) Celsius
CAV	Cardiac Allograft Vasculopathy
ConA	Concanavalin A
CR	Chronic Rejection
DSA	Donor-specific Antibody
ELISPOT	enzyme linked immunospot
H&E	hematoxylin and eosin
IFN	interferon
i.p	intraperitoneal(ly)
LN	lymph node
MLR	mixed lymphocyte reaction
MST	mean survival time
NK	natural killer
NKT	natural killer T [cell]
POD	postoperation day
Tg	transgene, transgenic
wk	week(s)

References

1. Meier-Kriesche HU, Schold JD, Kaplan B. Long-term renal allograft survival: Have we made significant progress or is it time to rethink our analytic and therapeutic strategies? Am J Transplant. 2004; 4:1289–1295. [PubMed: 15268730]
2. Meier-Kriesche HU, Schold JD, Srinivas TR, Kaplan B. Lack of improvement in renal allograft survival despite a marked decrease in acute rejection rates over the most recent era. Am J Transplant. 2004; 4:378–383. [PubMed: 14961990]
3. Kwun J, Knechtle SJ. Overcoming chronic rejection-can it B? Transplantation. 2009; 88:955–961. [PubMed: 19855237]
4. Terasaki PI. The review by Kwun and Knechtle-”can it B?”-asks whether B cells are responsible for chronic rejection of transplants. Transplantation. 2009; 88:978–979. [PubMed: 19855242]
5. Terasaki PI, Cai J. Human leukocyte antigen antibodies and chronic rejection: From association to causation. Transplantation. 2008; 86:377–383. [PubMed: 18698239]
6. Solez K, Colvin RB, Racusen LC, et al. Banff 07 classification of renal allograft pathology: Updates and future directions. Am J Transplant. 2008; 8:753–760. [PubMed: 18294345]
7. Tan CD, Baldwin WM 3rd, Rodriguez ER. Update on cardiac transplantation pathology. Arch Pathol Lab Med. 2007; 131:1169–1191. [PubMed: 17683180]
8. Girnita AL, McCurry KR, Zeevi A. Increased lung allograft failure in patients with HLA-specific antibody. Clin Transpl. 2007; 21:231–239.

9. Racusen LC, Colvin RB, Solez K, et al. Antibody-mediated rejection criteria – an addition to the Banff 97 classification of renal allograft rejection. Am J Transplant. 2003; 3:708–714. [PubMed: 12780562]
10. Mao Q, Terasaki PI, Cai J, et al. Extremely high association between appearance of HLA antibodies and failure of kidney grafts in a five-year longitudinal study. Am J Transplant. 2007; 7:864–871. [PubMed: 17391129]
11. Chow LH, Huh S, Jiang J, Zhong R, Pickering JG. Intimal thickening develops without humoral immunity in a mouse aortic allograft model of chronic vascular rejection. Circulation. 1996; 94:3079–3082. [PubMed: 8989111]
12. Russell PS, Chase CM, Winn HJ, Colvin RB. Coronary atherosclerosis in transplanted mouse hearts. II. Importance of humoral immunity. J Immunol. 1994; 152:5135–5141. [PubMed: 8176230]
13. Skaro AI, Liwski RS, Zhou J, Vessie EL, Lee TD, Hirsch GM. CD8+ T cells mediate aortic allograft vasculopathy by direct killing and an interferon-gamma-dependent indirect pathway. Cardiovasc Res. 2005; 65:283–291. [PubMed: 15621057]
14. Vessie EL, Hirsch GM, Lee TD. Aortic allograft vasculopathy is mediated by CD8(+) T cells in Cyclosporin A immunosuppressed mice. Transpl Immunol. 2005; 15:35–44. [PubMed: 16223671]
15. Knechtle SJ, Pascual J, Bloom DD, et al. Early and limited use of tacrolimus to avoid rejection in an alemtuzumab and sirolimus regimen for kidney transplantation: Clinical results and immune monitoring. Am J Transplant. 2009; 9:1087–1098. [PubMed: 19344431]
16. Willicombe M, Roufosse C, Brookes P, et al. Antibody-mediated rejection after alemtuzumab induction: Incidence, risk factors, and predictors of poor outcome. Transplantation. 2011; 92:176–182. [PubMed: 21637139]
17. Cai J, Terasaki PI, Bloom DD, et al. Correlation between human leukocyte antigen antibody production and serum creatinine in patients receiving sirolimus monotherapy after Campath-1H induction. Transplantation. 2004; 78:919–924. [PubMed: 15385814]
18. Gilliland LK, Walsh LA, Frewin MR, et al. Elimination of the immunogenicity of therapeutic antibodies. J Immunol. 1999; 162:3663–3671. [PubMed: 10092828]
19. Corry RJ, Winn HJ, Russell PS. Primarily vascularized allografts of hearts in mice. The role of H-2D, H-2K, and non-H-2 antigens in rejection. Transplantation. 1973; 16:343–350. [PubMed: 4583148]
20. Aperio Technologies. [Accessed April 9, 2012] Aperio | Support | Documentation. 2011. [cited July 26, 2011]; Available at: http://www.aperio.com/documents/
21. Aperio Technologies. [Accessed April 9, 2012] Image Analysis | Aperio. 2011. [cited July 26, 2011]; Available at: http://www.aperio.com/imageanalysis/image-analysis.asp
22. Kwun J, Knechtle SJ, Hu H. Determination of the functional status of alloreactive T cells by interferon-gamma kinetics. Transplantation. 2006; 81:590–598. [PubMed: 16495808]
23. Nagano H, Mitchell RN, Taylor MK, Hasegawa S, Tilney NL, Libby P. Interferon-gamma deficiency prevents coronary arteriosclerosis but not myocardial rejection in transplanted mouse hearts. J Clin Invest. 1997; 100:550–557. [PubMed: 9239401]
24. Koglin J, Glysing-Jensen T, Gadiraju S, Russell ME. Attenuated cardiac allograft vasculopathy in mice with targeted deletion of the transcription factor STAT4. Circulation. 2000; 101:1034–1039. [PubMed: 10704172]
25. van Besouw NM, Daane CR, Vaessen LM, Mochtar B, Balk AH, Weimar W. Donor-specific cytokine production by graft-infiltrating lymphocytes induces and maintains graft vascular disease in human cardiac allografts. Transplantation. 1997; 63:1313–1318. [PubMed: 9158027]
26. Tellides G, Tereb DA, Kirkiles-Smith NC, et al. Interferon-gamma elicits arteriosclerosis in the absence of leukocytes. Nature. 2000; 403:207–211. [PubMed: 10646607]
27. Gareau A, Hirsch GM, Lee TD, Nashan B. Contribution of B cells and antibody to cardiac allograft vasculopathy. Transplantation. 2009; 88:470–477. [PubMed: 19696629]
28. Kwun J, Bulut P, Kim E, et al. The role of B cells in solid organ transplantation. Semin Immunol. 2011; 24:96–108. [PubMed: 22137187]

29. Knechtle SJ, Pirsch JDH, Fechner JJ, et al. Campath-1H induction plus rapamycin monotherapy for renal transplantation: Results of a pilot study. Am J Transplant. 2003; 3:722–730. [PubMed: 12780564]

30. Nurieva RI, Chung Y, Hwang D, et al. Generation of T follicular helper cells is mediated by interleukin-21 but independent of T helper 1, 2, or 17 cell lineages. Immunity. 2008; 29:138–149. [PubMed: 18599325]

31. Chung Y, Tanaka S, Chu F, et al. Follicular regulatory T cells expressing Foxp3 and Bcl-6 suppress germinal center reactions. Nat Med. 2011; 17:983–988. [PubMed: 21785430]

32. Linterman MA, Pierson W, Lee SK, et al. Foxp3 +follicular regulatory T cells control the germinal center response. Nat Med. 2011; 17:975–982. [PubMed: 21785433]

33. Wu HY, Quintana FJ, Weiner HL. Nasal anti-CD3 antibody ameliorates lupus by inducing an IL-10-secreting CD4+ CD25− LAP+ regulatory T cell and is associated with down-regulation of IL-17+ CD4+ ICOS+ CXCR5+ follicular helper T cells. J Immunol. 2008; 181:6038–6050. [PubMed: 18941193]

34. Oliver AM, Martin F, Kearney JF. Mouse CD38 is down-regulated on germinal center B cells and mature plasma cells. J Immunol. 1997; 158:1108–1115. [PubMed: 9013949]

35. Flynn JM, Byrd JC. Campath-1H monoclonal antibody therapy. Curr Opin Oncol. 2000; 12:574–581. [PubMed: 11085457]

36. Lang G, Wotton D, Owen MJ, et al. The structure of the human CD2 gene and its expression in transgenic mice. Embo J. 1988; 7:1675–1682. [PubMed: 2901953]

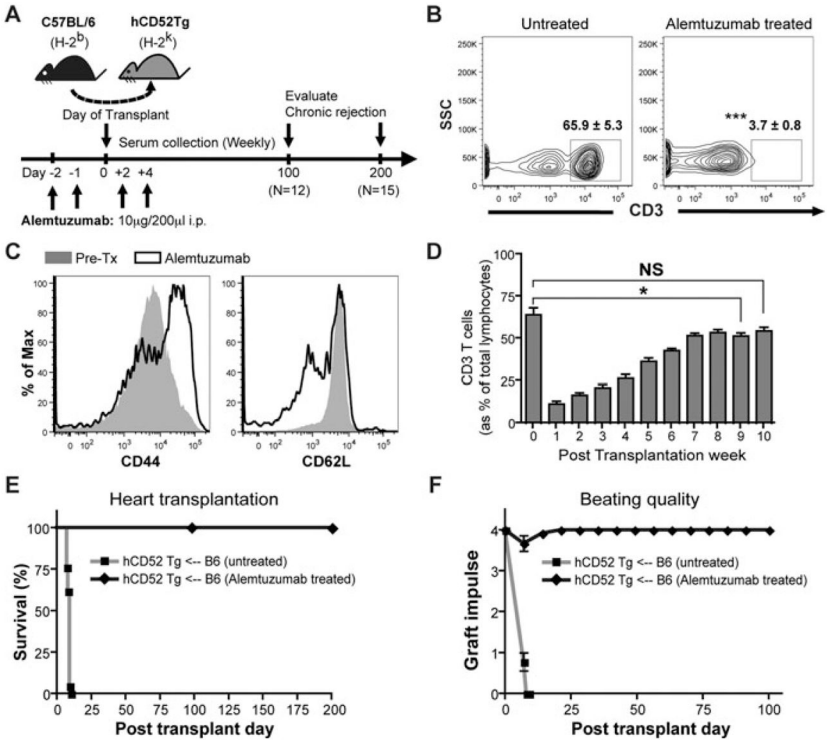

Figure 1. Alemtuzumab treatment induces prolonged full MHC mismatched cardiac allograft survival with profound T cell depletion in CD52Tg murine recipients

(A) Alemtuzumab dosing strategy and experiment are represented. C57BL/6 (H-2^b) hearts were transplanted into the CD52Tg mice (H-2^k). Recipients were treated with total four doses of 10 μg of alemtuzumab. (B) Representative dot plots of T cells in the peripheral blood before and after alemtuzumab treatment. Flow cytometric measurements demonstrated profound depletion of CD3 T cells on day 0 (in the gate) in the peripheral blood. The numbers depict the average percent (±SEM). n = 4 – 5 mice per group. (C) Phenotypic analysis of T cells during repopulation. Repopulating T cells showed phenotypic switching from $CD44^{lo}CD62L^{hi}$ (grey area) to $CD44^{hi}CD62^{lo}$ (solid line) population. (D) T cell repopulation kinetics after alemtuzumab treatment with cardiac allograft. Serial frequencies of repopulating T cells were expressed as percent of T cells ($CD3^+$) and of total lymphocytes ($CD45^+$). n = 5 – 7 mice per time point. (E) Cardiac allograft survival was prolonged with alemtuzuamab treatment (MST > 100 days, n = 12 and MST > 200 days, n = 15) while untreated recipients showed acute rejection at MST of 8.0 days (n = 12). (F) Posttransplant graft function measured by abdominal palpation (grade 0–4). Strong 3–4+ graft beating was maintained in alemtuzumab treated recipients until day 200, whereas beating quality dropped to less than 2+ within 7 days after transplantation and stop completely in untreated recipients. n = 12 per group. $^*p < 0.05$, $^{***}p < 0.001$, *NS* > 0.05.

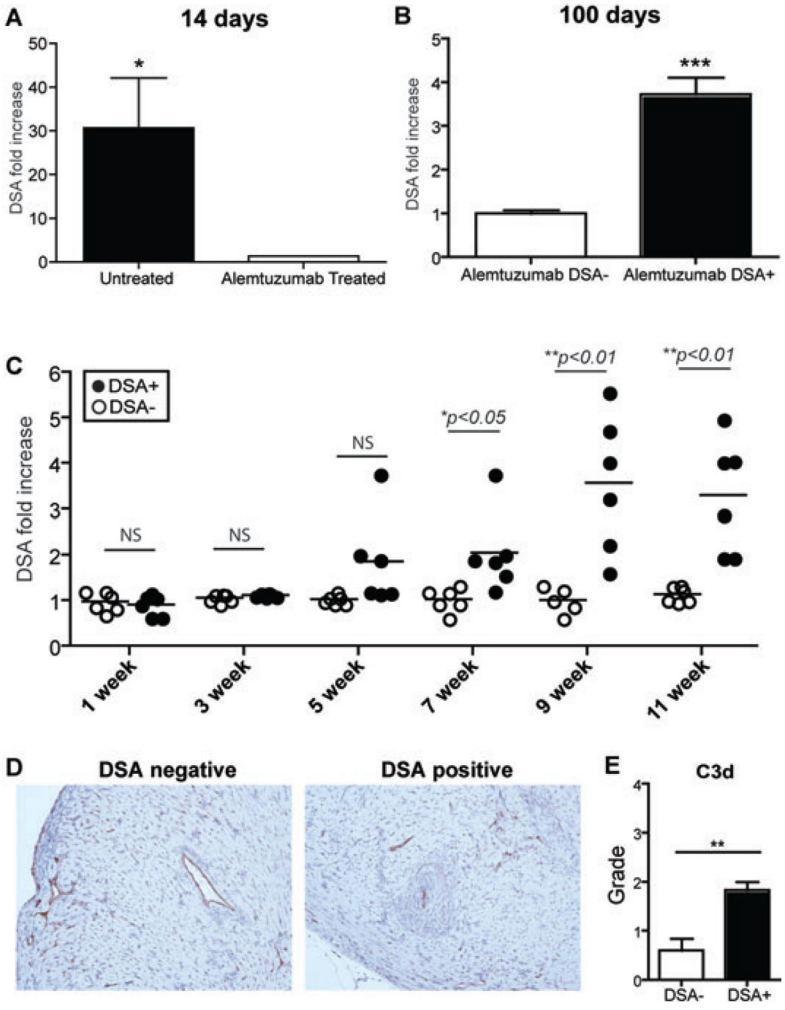

Figure 2. Patterns of serum alloantibody production after alemtuzumab treatment

Serum samples were recovered on the indicated days post-transplantation. 1×10^6 C57BL/6 donor splenocytes were used for cross-match. Pretransplant serum sample was used for fold increase. (A) Complete suppression of early alloantibody production after alemtuzumab treatment. DSA titer was increased in untreated recipients while no signs of alloantibody was found at 2 weeks posttransplant day in alemtuzumab treated recipients (n = 6 per group). (B) Partial suppression of late alloantibody production after alemtuzumab treatment. Fifty percent of recipients showed more than twofold increased DSA titer while the other half showed less than twofold increase (n = 6 per group). (C) Two DSA-producing phenotype after alemtuzumab treatment. Retrospective analysis of DSA+ versus DSA– serum samples showed differences as early as 7 weeks post-transplantation. Original magnification × 200. (D) Representative sections (n = 5~6) of explanted graft at day 100 from DSA+ and DSA– recipients with c3d immunohistochemistry for evaluation of antibody-mediated rejection. (E) C3d immunohistochemistry was scored semiquantitatively as 0, absent; 1, staining 1–10% of small capillaries; 2, staining 10–50% of small capillaries and 3, staining >50% of small capillaries. Grading for C3d deposition showed increased

level of C3d pathological deposition in DSA+ recipients (n = 6) compared to DSA– recipients (n = 5). $^{*}p < 0.05$, $^{**}p < 0.01$.

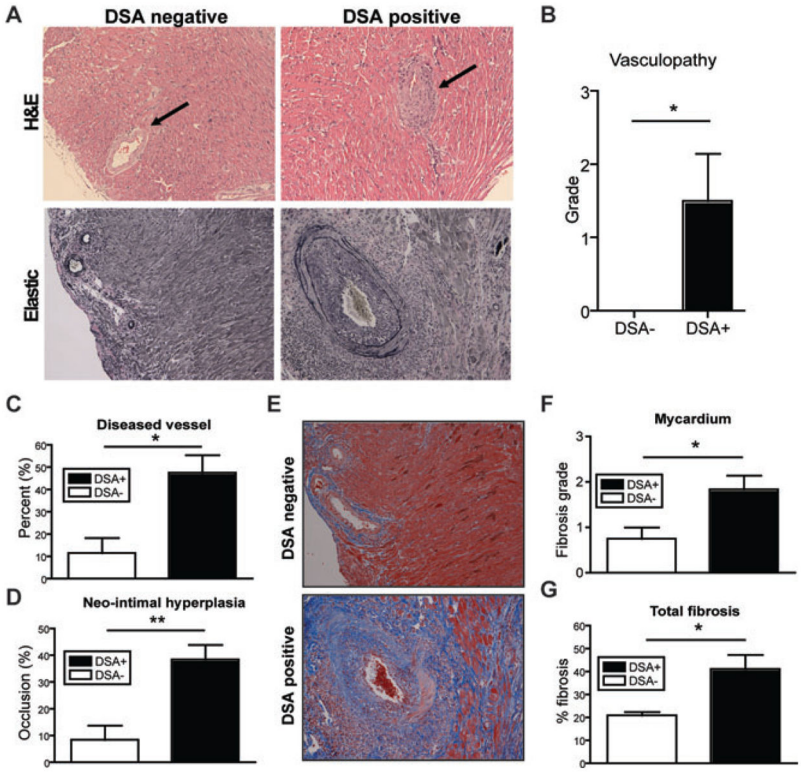

Figure 3. Histological analysis of representative graft tissue of DSA+ and DSA– recipients

(A) Representative sections of explanted graft at day 100 from DSA+ and DSA– recipients were stained with H&E and elastic staining for evaluation of CAV. Note the significant vasculopathy (arrow) in the DSA+ recipients and, in contrast, the relatively normal vascular integrity in the DSA– recipients at 100 days after transplantation. Original magnification ×200. (B) Vasculopathy was scored on elastic stains as 0, none; 1, mild, 0–10% of the luminal area compromised; 2, moderate, 10–50% of the luminal area compromised and 3, severe, greater than 50% of the luminal area compromised. Higher degrees of vasculopathy were identified in the graft from DSA+ recipients compared to DSA– recipients. (C) Morphometric analysis demonstrated more narrowing of vascular lumina in DSA+ recipients 100 days after transplantation than DSA–recipients. (D) Vessels showing more than 20% of occlusion were counted as diseased vessels. DSA+ recipients showed increased number of diseased vessels at day 100. (E) Representative of trichrome stained grafts showed the diffuse fibrosis and thickened vascular wall (stained blue), consistent with CAV. (F) Fibrosis was semi-quantitatively scored in the myocardium as 0, none; 1, 0–10%; 2, 10–50% and 3, >50% of the myocardial area. Increased level of fibrosis in myocardial area of DSA+ recipients was identified compared to DSA–recipients. Original magnification ×200. (G) Total fibrosis measured from entire explanted graft showed significantly increased in DSA+ recipients compared to DSA– recipients. The percentage of total fibrosis was quantified and expressed as% positive trichrome pixels. Data here are expressed as mean ± SEM of six grafts in each group. $^{*}p < 0.05$, $^{**}p < 0.01$.

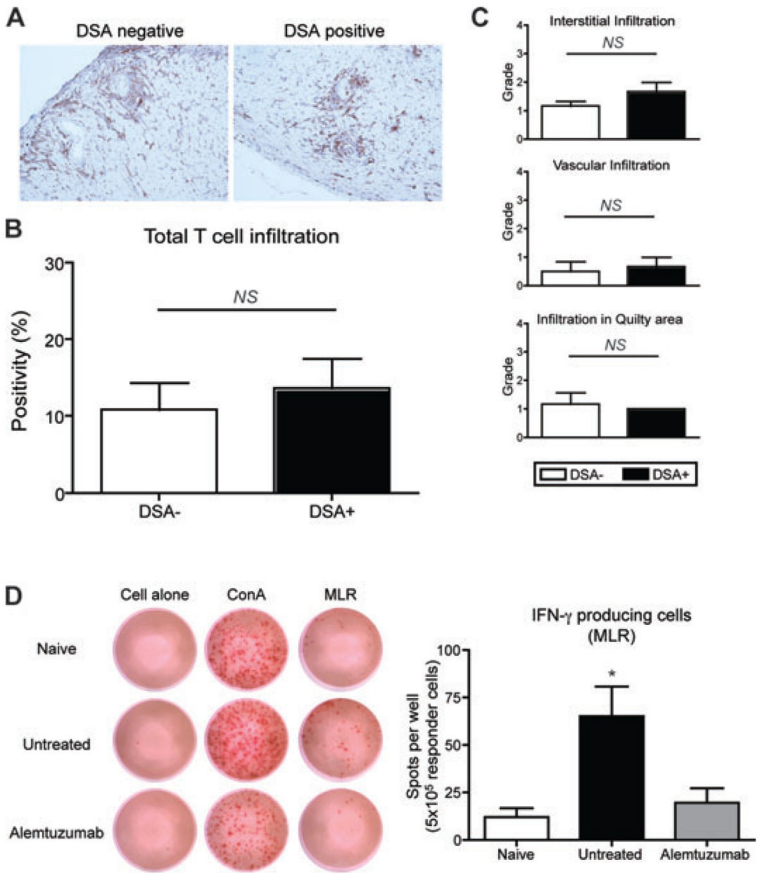

Figure 4. Allospecific T cells in long-term recipients

A. Representative section of graft from DSA+ and DSA– recipients with alemtuzumab treatment, 100 days after transplantation (CD3 immunohistochemistry). Note the minimal perivascular infiltration of T cells in the graft for both DSA+ and DSA– group without parenchymal rejection. Original magnification ×200. (B) The quantification of T cell infiltration showed similar level of intragraft T cell infiltration (n = 5 per group). (C) Grading of T cell infiltration in different graft compartments showed no difference on T cell infiltration in interstitial, vascular and quilty area (n = 6 per group). (D) IFN-γ producing cells detected by ELISPOT. Splnocytes derived from naïve, untreated and alemtuzumab treated recipients were cocultured with medium alone, ConA (5 μg/mL) or irradiated B6 splenocytes (5×10^6 cells). Splenocytes from alemtzumab treated recipient showed significantly less number of spot compared to cells from untreated recipients (n = 6 per group). *NS* > 0.05, $^{*}p < 0.05$.

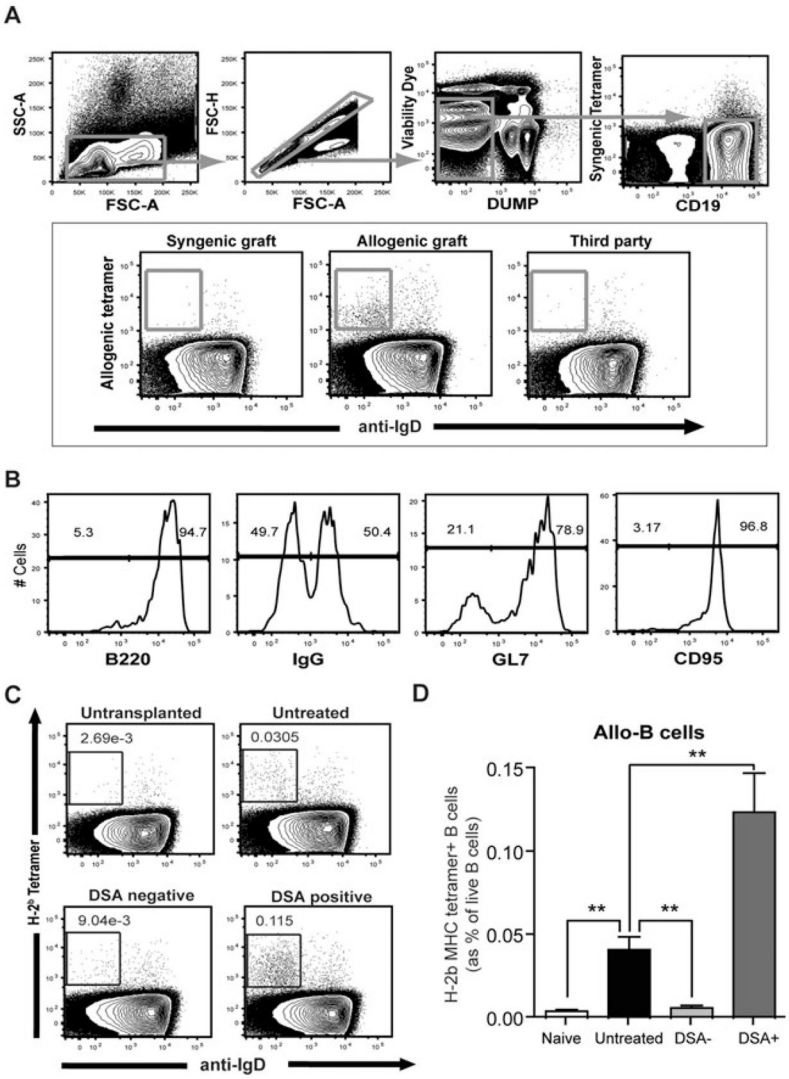

Figure 5. Visualization of alloreactive B cells after cardiac allograft

(A) Formation of allo-B cells was tracked with donor MHC tetramer (H-2K^b/D^b). Gating strategy for allo-reactive B cells was depicted schematically. Splenocytes from syngeneic, allogeneic and allogeneic third party recipients were evaluated. Allo-B cells were found only from allogeneic recipients' splenocytes. (B) Phenotype of donor MHC tetramer$^+$ B (Allo-B) cells was analyzed with B220, IgG, GL7 and CD95 mAbs. (C) Splenocytes from cardiac allograft recipients were analyzed after 100 days of transplantation. As a control, splenocytes from naïve CD52Tg mice were also evaluated. Dot plots of live B cells were depicted and show the IgD (x-axis) profile of cells stained with donor MHC tetramer (y-axis). (D) Increased allo-reactive (anti-K^b/D^b) B cells were identified from untreated and DSA+ recipients. Allo-B cell levels of DSA– recipients showed no difference from those of naïve mice. Allo-B cell levels were significantly higher in DSA+ recipients compared to untreated recipients (n = 5 per each group). $^{**}p < 0.01$.

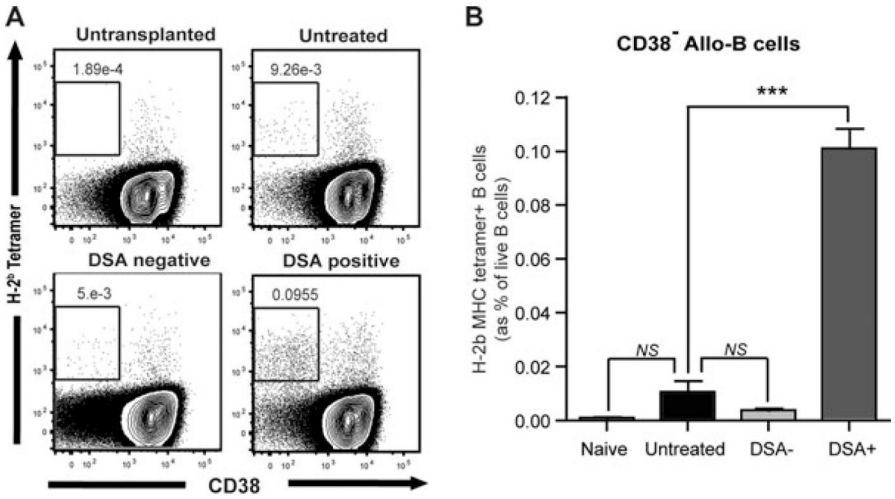

Figure 6. Distinct allo-B cell repertoire in chronic rejection

(A) Splenocytes from cardiac allograft recipients were analyzed 100 days after transplantation. As a control, splenocytes from naïve CD52Tg mice were also evaluated. Dot plots of live B cells were depicted and show the CD38 expression (x-axis) profile of cells stained with donor MHC tetramer (y-axis). (B) Increased $CD38^{-}$ allo-reactive (anti-K^b/D^b) B cells were only identified from DSA+ recipients (n = 4 per each group). $^{***}p < 0.001$.

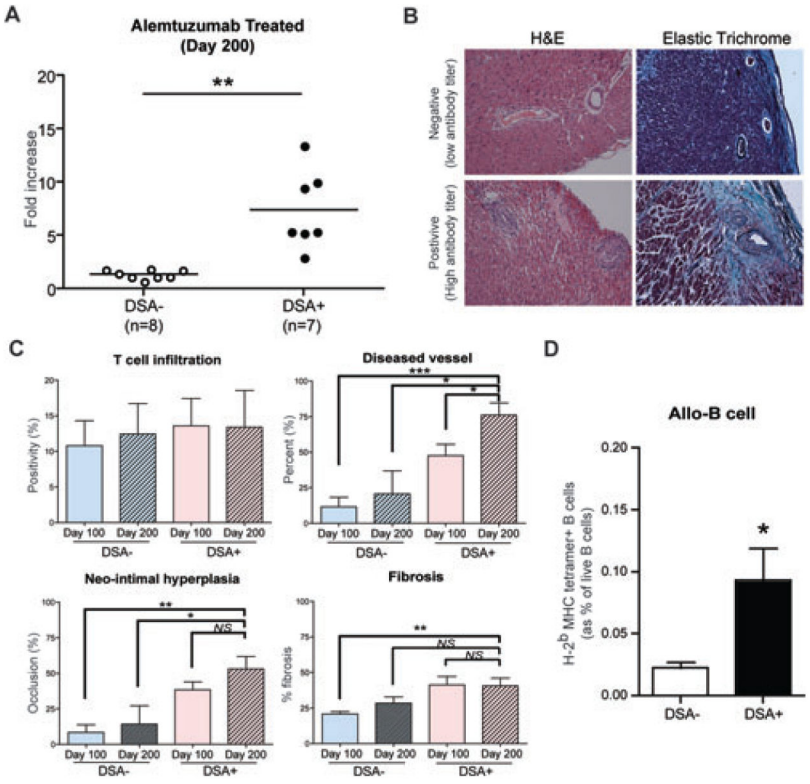

Figure 7. Alloantibody production and chronic rejection development in alemtuzumab treated CD52Tg recipients at day 200

(A) Serum alloantibody detection with flow crossmatch showed two distinct phenotypes either with low alloantibody titer (negative) or with high alloantibody titer (positive). (B) Representative sections of explanted graft at day 200 from DSA+ and DSA– recipients were stained with H&E and elastic trichrome staining for evaluation of CAV. Original magnification ×200. (C) The quantification of T cell infiltration showed similar level of intragraft T cell infiltration in all groups. DSA+ recipients showed increased number of diseased vessel at day 200. Mophometric analysis demonstrated only a trend of increased neo-intimal hyperplasia in DSA+ recipients at 200 days after transplantation than DSA– recipients. Total fibrosis measured from entire explanted graft showed no difference in DSA + recipients compared to DSA– recipients. Data are expressed as mean ± SEM of six grafts in each group. (D) The DSA+ recipients (n = 7) showed significantly increased levels of alloreactive (anti-K^b/D^b) B cells in the spleen compared to DSA– recipients (n = 8). *NS* > 0.05, $^{*}p < 0.05$, $^{**}p < 0.01$, $^{***}p < 0.001$.